Screening and impurity removal device to improve the accuracy of moisture content detection device for rice

Han Tang[1], Changsu Xu[1], Jiale Zhao[2], Yijia Wang[3*]

(1. *College of Engineering, Northeast Agricultural University, Harbin 150030, China*;
2. *College of Biological and Agricultural Engineering, Jilin University, Changchun 130025, China*;
3. *Department of Industrial and Manufacturing Systems Engineering, The University of Hong Kong, Pokfulam Road 999077, China*)

Abstract: An online detection device that used the capacitance method to detect the moisture content of rice in a combine harvester was designed and found a low detection accuracy because of the high impurity content of the samples.　To solve this problem, a screening and impurity removal device was designed in this study, and the structural parameter range of the screw conveyor was the focus of the design.　To determine the best structural parameters and operating parameters of the device, models of rice grains and short stems were established by the discrete element method.　The Discrete Element Method (DEM) simulation test was carried out according to the Box-Behnken response surface method.　When the rotating speed was 300 r/min, the diameter of spiral blade was 146 mm, the pitch was 80 mm, the diameter of rotating shaft was 30.6 mm, and the minimum impurity content was 0.27%.　The density distributions and movement characteristics of the rice grains and short stems in the optimized screening and impurity removal device were studied.　An experiment was carried out to compare data for the moisture content of rice measured by the online moisture content detection device before and after the installation of the screening and impurity removal device and the results of the 105 ℃ drying method.　The results showed that the impurity content of rice ranged from 0.26% to 0.37%, and the maximum effective screening rate was 90.99% after screening.　The screening and impurity removal device significantly reduced the error in the moisture content measured by the online detection device, the error range was 0.12%-2.55%.　This study provides a method for accurate online detection of moisture content and provides a reference for the design and simulation of related screening devices.

Keywords: combine harvester, parameter optimization, rice, motion characteristics, discrete element model

DOI: 10.25165/j.ijabe.20221506.7299

1　Introduction

Rice is one of the main food crops in the world, and the moisture content of rice is a key index for its safe storage, production and processing[1].　Excessive moisture content can easily cause grain germination, mildew, difficulties during storage and other problems that reduce its nutritional value and cause enormous economic losses[2].　Accurate online detection of moisture content is of great significance to ensure national food security and intelligent development of crop harvests[3,4].

Moisture content detection is generally divided into direct measurement and indirect measurement methods.　The direct measurement method removes moisture from materials by drying or chemical methods, and the absolute water content in the sample is determined.　This method changes the physical properties of the sample[5].　The indirect measurement methods mainly include the

microwave method, capacitance method, resistance method, infrared method, frequency domain method and neutron method[6,7].　Among them, the capacitance method measures moisture content according to the dielectric constant of the material, which has the advantages of low cost, fast detection, and little damage to the sample; it has been widely studied[8].　At present, the capacitance method is the primary method used in nondestructive testing of fruit and vegetable quality[9,10].　Liu et al.[11] used dielectric properties to evaluate the non-destructive sugar content of several melon varieties.　Wang et al.[12] collected the electrical indexes of several apples with watercourse disease and developed an instrument for nondestructive detection of apple lesions.　In addition, relevant scholars also applied the capacitance method to detect moisture in food crops[13,14].　Based on the principle of the noncontact parallel plate capacitance measurement, Mai et al.[15] developed a grain moisture detection device suitable for harsh environments.　Wan et al.[16] studied the parallel plate capacitor and adopted the fin-shaped double-plate detection method to optimize a detection device for rice moisture content.　In the above study, the online detection device was directly installed in the grain tank after harvest.　However, a large number of short stems and other residues were carried with the grain during the harvest period.　Relevant studies[17] showed that impurities had a significant impact on the detection accuracy when the capacitance method was used to detect the moisture content of grain crops.

At present, the screening device is mainly configured in the cleaning part of the combine harvester, which is used in combination with the fan to separate the grains and impurities by

throwing, dispersing and layering the mixture[18].   Work is underway to develop the screening device, increase its efficiency and cleanliness and reduce losses, but there are still some short stems among the harvested grains that interfere with the detection accuracy of water content.   At the same time, the screening device is a planar structure, and its motion form, layout scheme and impurity content accuracy are significantly different from the requirements of the screening and impurity removal device configured in front of the moisture content detection device.   The current method and theoretical research have little relevance for reference, and cleaning screens cannot be replaced directly.   There is no report of configuring impurity removal devices for use in front of moisture detection devices.

Rice grains and short stems can be regarded as a complex system with inherent organic relationships through the interaction of many discrete particles[19].   The interactions and motion mechanism cannot be explored effectively.   In recent years, the discrete element method (DEM) developed by Cundall has become an effective means to study the dynamics of granular particles; it can track the motion of each particle and predict the detailed dynamic process of a particle group by using energy exchange between the particles and collisions between the particles and the boundary.   At present, the computational efficiency and simulation accuracy of this method have been improved, and now it can calculate the motions of millions of particle in complex systems[20].

In this study, a screening and impurity removal device was designed on the basis of an online detection device for moisture content, and the optimal parameter combination of the screw conveyor was explored by the discrete element method and Box-Behnken response surface method.   The density distributions and movement characteristics of rice grains and short stems were analyzed in the optimized screening device, and the significant effect of the device on the detection accuracy of moisture content was verified by field experiments.   This study provides a method for online accurate detection of moisture content and a reference for the design and simulation of related screening devices.

2   Materials and methods

2.1   Overall structure and working principle

The online moisture content detection device of the combine harvester is mainly composed of a feeding hopper, sieve separator, grain gathering bucket, frame, grain row wheel, sample discarding motor, capacitance sensor, mass sensor, sampling motor, screw conveyor and so on, as shown in Figure 1.   The feeding hopper is mounted below the grain outlet of the combine harvester to ensure the adequate collection of grain samples.   The sampling motor drives the screw conveyor to rotate at a uniform speed, which can not only separate grains from impurities but also ensure the continuity and uniformity of sampling.

The workflow of the online moisture content detection device of the combine harvester is mainly divided into four stages: hopper feeding, screening, storage of grain to be tested, and uniform grain discharge by the grain row wheel.   When part of the grain is discharged into the hopper at the grain outlet of the combine harvester, the sampling motor drives the screw conveyor to collect a sample.   A sieve separator is used to screen the rice grains and short stems.   The short stems are removed through the other end of the sieve separator, and the rice grains fall freely from the grain bucket into the capacitance sensor for detection.   The sample discarding motor drives the grain row wheel to rotate at a uniform

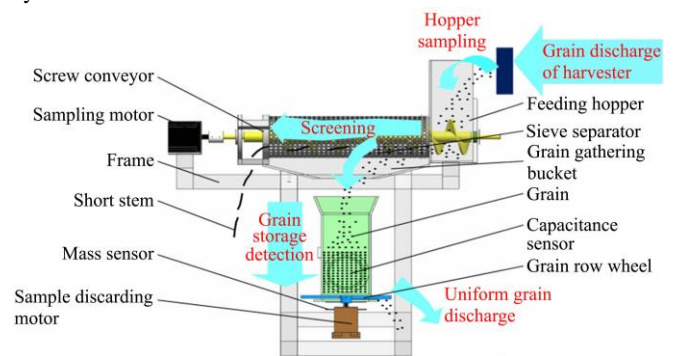speed to discharge the tested rice samples and complete a working cycle.

Figure 1   Online moisture content detection device of the combine harvester

The capacitance sensor mainly detects the overall moisture content according to the various capacitance values of the rice grains with different moisture content.   When the rice grains accumulate in the signal detection chamber, the sensor outputs the capacitance value[14].   However, the rice grains are mixed with a large number of short stems after harvest in a complex field environment.   The capacitance value of the mixture is significantly different from that of the rice grains, which seriously interferes with the detection of moisture content.   Therefore, the screening and impurity removal device can separate the rice grains from the short stems.   The rationality of the design directly affects the effectiveness and accuracy of the online moisture content detection device of the combine harvester.

2.2   Design of screening and impurity removal device

The screening and impurity removal device is mainly composed of a feeding hopper, sieve separation drum, grain gathering bucket, screw conveyor, sampling motor and so on, as shown in Figure 2.   Among them, the screw conveyor and the sieve separation drum are the core components of the screening and impurity removal device, and the rotating power of the screw conveyor is provided by the sampling motor.   Its structural parameters and operational parameters play a key role in separation, impurity removal and continuous transportation.

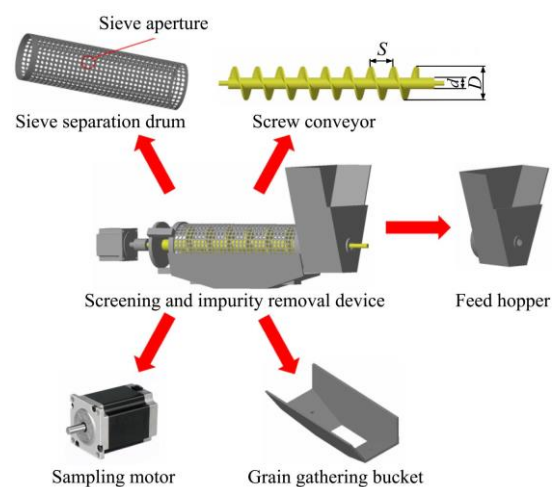Figure 2   Key components of the screening and impurity removal device

To avoid the entanglement of a large number of the short stems (mixed with the rice grains after harvest) on the rotation axis of the screw conveyor, the circumference of the rotation axis should be greater than the average length of the short stems.   The average length of the short stems was 92.23 mm in the grain tank after the

harvest in this study.   That is,

$$\pi d > l \qquad (1)$$

where, d is the diameter of the rotation axis, mm; l is the average length of the short stems; mm; l is 92.23 mm; and $d > 29.23$ mm.

Referring to the "design manual of nonstandard machinery and equipment", the relationship between the rotating shaft of the screw conveyor and the diameter of the screw blade is as follows:

$$d = (0.2\sim0.35)D \qquad (2)$$

where, D is the diameter of the helical blade, mm; and the diameter of the helical blade is 66.37 mm $< D < 146.15$ mm.

When the pitch is too large or too small, it can increase the occupied volume in the grain tank or reduce the separation efficiency, respectively.   To ensure the rapid removal of rice grains and the real-time detection of moisture content, the pitch should be moderate.   The equation of pitch is as follows:
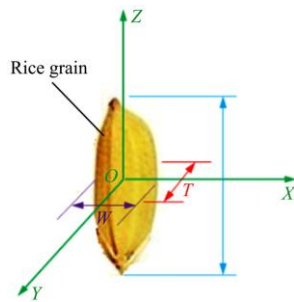
$$S = kD \qquad (3)$$

where, S is the pitch, mm; k is the material filling coefficient, and its value is related to the arrangement of the screw conveyor and the flow characteristics of the conveyed material.   According to the physical characteristics of short stems and rice grains, k is 0.3-0.6.   Then, the pitch is 19.91 mm $< S < 87.69$ mm.
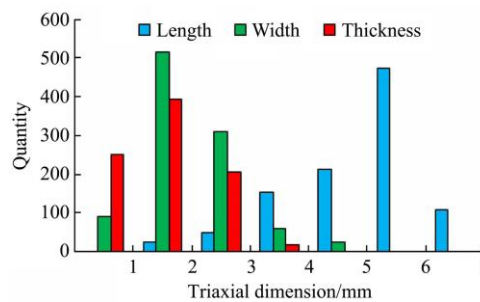
The conveying capacity of screw conveyer is as follows:

$$Q = 47(D^2 - d^2)Sn\gamma k \times 10^{-9} \qquad (4)$$

where, Q is the conveying capacity of the screw conveyor, kg/min; the grain flow rate of rice at the grain outlet of the combine harvester is 120 kg/min; then Q is 120 kg/min; γ is the bulk density of transporting rice, kg/m³, and γ is taken as 600 kg/min; n is the rotating speed of the screw conveyor, r/min, and n is 236.65 r/min

in this study.

The optional sampling motor is an 86D two-phase hybrid stepper motor (Shenzhen Vicote Electromechanical Co., Ltd., Shenzhen, China), and its maximum speed is 1000 r/min (adjustable), which meets the requirements of optimal design.

The sieve separator serves as the separation channel between the short stems and the rice grains, and it can screen the clean rice grains and deliver them to the capacitance sensor detection area. Taking Longjing 29, a rice widely planted in Northeast China, as the research object, 1000 rice grains were randomly selected at a suitable harvest time; their triaxial size was measured by using Vernier calipers (Shanghai Shoufeng Precision Instrument Co., Ltd., Shanghai, China) and a statistical analysis was carried out, as shown in Figure 3.   Among the results, the length (L), width (W) and thickness (T) of the rice grains were mainly distributed between 5-6 mm, 1-2 mm, and 1-2 mm, respectively; the average values were 5.63 mm, 2.05 mm and 1.80 mm, respectively.   The joint action of the screw conveyer, sieve separator and rice grains can change the movement and orientation of the short stems and prevent them from passing directly through the sieve holes into the signal detection chamber.   The short stems are significantly longer than the dimensions of the rice grains, and the size of the sieve apertures can be directly defined as the triaxial size of rice grains. To ensure that the rice grain can pass smoothly through the sieve apertures smoothly to improve the separation efficiency and reduce the impurity content, the diameter of the sieve aperture is more than 1.5 times the average length of the rice grains; the diameter of the sieve aperture is set to 8.5 mm in this study.

a. Characteristic size of a rice grain   b. Statistical diagram of the triaxial size distribution

Figure 3   Characteristic size and triaxial size distribution of the rice grains

2.3 Discrete element simulation experiment

To intuitively analyze the screening relationship of the structural parameters and operating parameters of the screw conveyor within the design range and determine the best design parameters, discrete element models of rice grains and short stems were accurately established by a three-dimensional laser scanning technique.   The Box-Behnken response surface method was used to design the experiment, EDEM 2018 software was used to explore the effects of different parameter combinations on the impurity content, and the optimal parameter combination of the screw conveyor was obtained.

2.3.1   Establishment of discrete element model

The overall structure of rice grain is complex.   To accurately establish a rice grain model, rice grains with approximate average triaxial sizes (5.58 mm, 2.05 mm and 1.83 mm) were selected. The three-dimensional geometric feature parameters of rice grains were extracted by a Reeyee X5 three-dimensional laser scanner (Nanjing Weibo 3D Technology Co., Ltd., Nanjing, China) that projects gratings onto the surfaces of rice grains.   The spatial coordinates of each point on the surface were accurately calculated by the orientation and triangulation methods.

Three-dimensional point cloud data were generated.   The operations, in turn, were shading, denoising, point cloud registration, point cloud triangulation, merging and model modification.   The scanning data were converted into accurate digital models by using automatic reverse engineering software, and the model of rice grain scanned by the three-dimensional laser was imported into the EDEM software[21-23].   The "spherical particle polymerization" method was used to fill the model[24], and the discrete element model of rice grain was established, as shown in Figure 4a.   The short stems were cylindrical in general.   The average length was 92.23 mm, and the average diameter was 5.11 mm.   The spherical particle polymerization method was used to fill the model, and the model of short stems was established, as shown in Figure 4b.   The feeding hopper, sieve separator and screw conveyor were all made of steel, and their discrete element models are shown in Figure 4c.   According to a related reference[25,26], the relevant simulation and contact parameters set are shown in Table 1.   To accurately express the contact characteristics between rice grains and short stems, the Hertz-Mindlin (no-slip) contact model was used to construct rice grains and short stems.
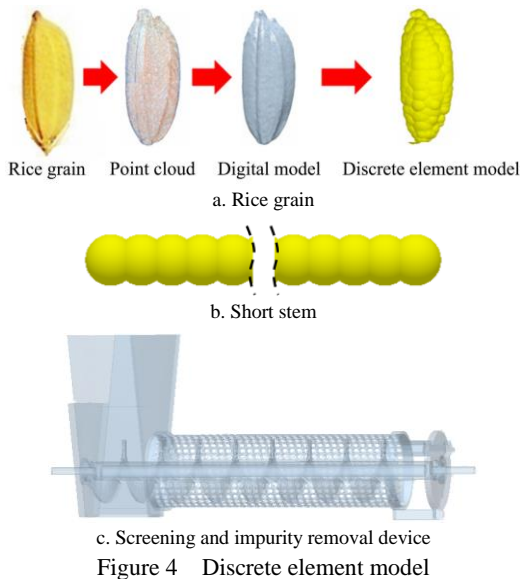
a. Rice grain

b. Short stem

c. Screening and impurity removal device

Figure 4   Discrete element model

Table 1   simulation and contact parameters

Parameter	Value		
Density/kg m^{-3}	1137[a]	623[b]	7800[c]
Shear modulus/Pa	8.24×10^{6}[a]	2.30×10^{5}[b]	7.00×10^{10}[c]
Poisson's ratio	0.3[a]	0.4[b]	0.3[c]
Static friction coefficient	0.61[aa] 0.35[ab] 0.34[bb] 0.31[bc]		0.34[ac]
Dynamic friction coefficient	0.02[aa] 0.02[ab] 0.02[bb] 0.01[bc]		0.01[ac]
Restitution coefficient	0.46[aa] 0.37[ab] 0.33[bb] 0.36[bc]		0.47[ac]

Note: a: Physical parameters of rice grain; b: Physical parameters of short stem; c: Physical parameters of steel; aa: Contact parameters between rice grains; ab: Contact parameters between rice grains and short stems; ac: Contact parameters between rice grains and steel; bb: Contact parameters between short stems; bc: Contact parameters between short stems and steel.

There was a certain initial speed in the transportation of rice grains and short stems from the inlet of the grain tank to the hopper in the combine during the harvest process.   The gravity acceleration was set to 9.81 m/s^2.   The "falling rain method" was used to make rice grains and short stems accumulate in the hopper at a ratio of 29:1, and the initial velocity was set to 1 m/s.   The time step was determined to be 15% by the Rayleigh method, and the total simulation time of each group was set to 25 s.   During postprocessing, counters of rice grains and short stems were used to calculate the effects of structural parameters and operating parameters on the index of impurity content.

2.3.2   Experimental design

To explore the influence of screw conveyor structure parameters and operation parameters on impurity content in the screening process, rotating speed, helical blade diameter, pitch and rotating shaft diameter were selected as experimental factors, and screening impurity content was selected as the performance index. The Box-Behnken response surface method was used to design the experiment, and the related experiments were carried out by EDEM 2018 software.   The impurity content was calculated by Equation (5).   The horizontal coding table of the experimental factors is listed in Table 2.

Table 2   Horizontal coding table of Box-Behnken experimental factors

Level	Rotating speed x_1/r min^{-1}	Helical blade diameter x_2/mm	Pitch x_3 /mm	Rotating shaft diameter x_4/mm
−1	240	70	20	30
0	270	108	50	45
1	300	146	80	60

$$y = \frac{W_z}{W} \times 100\% \qquad (5)$$

where, y is the impurity content,%; W_z is the total mass of short stems dropped by the sieve separator, g; and W is the total mass of rice grains and short stems transported by the screening and impurity removal device, g.

2.4   Field experiment

To verify the rationality of the design of the screening and impurity removal device, the effectiveness and accuracy of the online moisture content detection device were tested at the same time.   The rice harvest field experiment was carried out in the experimental rice field of the Intelligent Paddy Field Agricultural Equipment and Technology Team of Northeast Agricultural University in Qingan County, Suihua City, Heilongjiang Province from October 2 to 5, 2020, as shown in Figure 5.   The rice variety was Longjing 29, which had the following natural properties: the height was 73.3 cm, the 1000-grain weight was 37.7 g, and the grain-grass ratio was 1.06 g.   The optimized screening and impurity removal device was installed at the grain tank inlet of a CF805N full-feeding combine harvester (Jiangsu Changfa Agricultural Equipment Co., Ltd, Changzhou, China) with a cutting width of 2 m and a stubble height of 15 cm.   The grain moisture content was 13.56% to 19.93%.

a. Experimental prototype

b. Installation location

Figure 5   Field experiment

A flat field was selected, and the rice stood upright without tilting before the experiment.   The path length was 35 m, and crops in a row of width 5 m were reserved before each experiment to ensure that the harvester worked with a consistent feeding quantity before entering the experimental area[27].   The rated driving speed of the combine harvester was 3.2 km/h.   As the moisture content of rice varied with harvest time, the rice moisture content detection device was tested for 4 d to evaluate the rice moisture content under different moisture content conditions.   The daily working times of the experiment were 8:00, 10:00, 12:00, 14:00, 16:00 and 18:00.   Each group of experiments was repeated three times, and the average value of the three results was taken as the effective value of this period of time.

To accurately compare the performance of the screening device to separate short stems and residues, the impurity contents of rice with and without processing by the screening device were compared and analyzed.   Rice weighing 30 kg was selected in the

grain tank, and the short stems and residues before and after screening were manually screened and weighed.   The impurity content of rice was calculated by Equation (5).   The effective screening rate is used to measure the screening capacity of the screening and impurity removal device by Equation (6).

$$S = \frac{I_1 - I_2}{I_1} \times 100\% \qquad (6)$$

where, S is the effective screening rate,%; I_1 is the impurity content before screening, %; and I_2 is the impurity content after screening, %.

To examine the influence of the screening and impurity removal device on the performance of the online moisture content detection device, the moisture contents measured by the online detection devices without and with the operation of the screening and impurity removal device were compared with the moisture content measured by the drying method at 105°C[28].   The instrument used in the 105°C drying method was a DZF-6051 electric blast drying oven (Qingdao Mingbo Environmental Protection Technology Co., Ltd., Qingdao, China).   The rice grain was put into an aluminum box for measurement.   The mass of the rice before drying was measured, and it was put in the drying box. The aluminum box was placed in the oven at 105°C for 4 h without interruption.   The aluminum box was removed, and the mass of the rice after drying was determined.   The moisture content of rice grains was calculated by Equation (7).

$$C = \frac{M_1 - M_2}{M_1} \times 100\% \qquad (7)$$

where, C is the moisture content of the rice grains,%; M_1 is the mass of the undried rice grains, g; and M_2 is the mass of the rice grains after drying, g.

3   Results and discussion

3.1   Effect of structural parameters and operating parameters on impurity content

According to the coding table of experimental factors, the Box-Behnken experiment was designed by Design-Expert software, and 29 experimental sites were designed for analysis.   The Box-Behnken experimental scheme and results are listed in Table 3.

According to the experimental scheme in Table 3, the multiple regression fitting analysis and variance analysis were carried out by using Design-Expert 8.0.6 software, and the F-test was carried out on the experimental factors and regression model.   The results are listed in Table 4.

As shown in Table 4, the primary and secondary experimental factors that influenced impurity content y were x_4, x_2, x_3 and x_1. Among them, $p<0.01$ for x_2, x_3, x_4, x_2x_3, x_2^2, and x_4^2, and these factors had a significant effect on the impurity content. Additionally, $p<0.05$ for x_2x_4, x_3x_4, and x_3^2, and these factors had a significant effect on the impurity content.   For other factors, $p>0.05$, and the effect of these factors on impurity content was nonsignificant.   After removing the insignificant quadratic term, the quadratic multiple regression model obtained by fitting was as follows:

$$y = 1.22 + 0.02x_1 - 0.35x_2 - 0.21x_3 - 0.38x_4 - 0.35x_2x_3 - 0.083x_2x_4 - 0.082x_3x_4 + 0.098x_2^2 - 0.062x_3^2 + 0.11x_4^2 \qquad (8)$$

The results of the regression model were $F=73.61$ and $p<0.0001$, which showed that the model was significant.   The determination coefficient R^2 of the impurity content y was 0.9244, which showed that the regression model explained 92.44% of the variability of the experimental data.   The correction determination coefficient R^2_{adj} was 0.9732, which showed that the four selected

factors determined the change in moisture content of approximately 97%.   The predicted value of the regression model was highly correlated with the actual value, and the experimental error was small.

Table 3   Box-Behnken experimental scheme

Order	Rotating speed x_1/r min^{-1}	Helical blade diameter x_2/mm	Pitch x_3 /mm	Rotating shaft diameter x_4/mm	Impurity content y/%
1	−1	−1	0	0	1.66
2	1	−1	0	0	1.20
3	−1	1	0	0	1.24
4	1	1	0	0	1.21
5	0	0	−1	−1	1.71
6	0	0	1	−1	0.27
7	0	0	−1	1	1.53
8	0	0	1	1	0.96
9	−1	0	0	−1	2.05
10	1	0	0	−1	1.71
11	−1	0	0	1	0.95
12	1	0	0	1	1.57
13	0	−1	−1	0	0.65
14	0	1	−1	0	1.58
15	0	−1	1	0	0.90
16	0	1	1	0	0.91
17	−1	0	−1	0	1.32
18	1	0	−1	0	1.27
19	−1	0	1	0	1.25
20	1	0	1	0	1.55
21	0	−1	0	−1	1.73
22	0	1	0	−1	1.41
23	0	−1	0	1	0.91
24	0	1	0	1	0.97
25	0	0	0	0	1.74
26	0	0	0	0	1.22
27	0	0	0	0	1.62
28	0	0	0	0	1.17
29	0	0	0	0	0.66

Table 4   Results of analysis of variance

Variance source	Impurity content y				
	Squares sum of partial square differences	Freedom	Mean square	F	p	Significance
x_1	0.0048	1	0.0048	1.11	0.3101	*
x_2	1.44	1	1.44	331.68	<0.0001	***
x_3	0.53	1	0.53	121.33	<0.0001	***
x_4	1.72	1	1.72	396.95	<0.0001	***
x_1x_2	0.0049	1	0.0049	1.13	0.3053	*
x_1x_3	0.0004	1	0.0004	0.092	0.7656	*
x_1x_4	0.0049	1	0.0049	1.13	0.3053	*
x_2x_3	0.5	1	0.5	116.50	<0.0001	***
x_2x_4	0.027	1	0.027	6.29	0.0251	**
x_3x_4	0.027	1	0.027	6.29	0.0251	**
x_1^2	0.006993	1	0.006993	1.62	0.2244	*
x_2^2	0.063	1	0.063	14.52	0.0019	***
x_3^2	0.025	1	0.025	5.69	0.0318	**
x_4^2	0.085	1	0.085	19.71	0.0006	***
Sum of model residual misfit error	4.46	14	0.32	73.61	<0.0001	***
	0.061	14	0.004327			
	0.059	10	0.005886	13.69	0.0112	
	0.00172	4	0.00043			
	4.52	28				

Note: $p<0.01$ means extremely significant (***), $p<0.05$ means significant (**), $p>0.05$ means nonsignificant (*).

Table 4 shows that the interaction of the experimental factors had a certain influence on the experimental index.   Among them, x_2x_3, x_2x_4, and x_3x_4 had a great influence on moisture content. However, x_1x_2, x_1x_3, and x_1x_4 had little influence on moisture

content.   To explore the influence level and trend of the interaction of various factors on moisture content, an interactive response surface diagram of each factor was established, as shown in Figure 6.

a. Influence of rotating speed and helical blade diameter on impurity content

b. Influence of rotating speed and pitch on impurity content

c. Influence of rotating speed and rotating shaft diameter on impurity content

d. Influence of helical blade diameter and pitch on impurity content

e. Influence of helical blade diameter and rotating shaft diameter on impurity content

f. Influence of rotating shaft diameter and pitch on impurity content
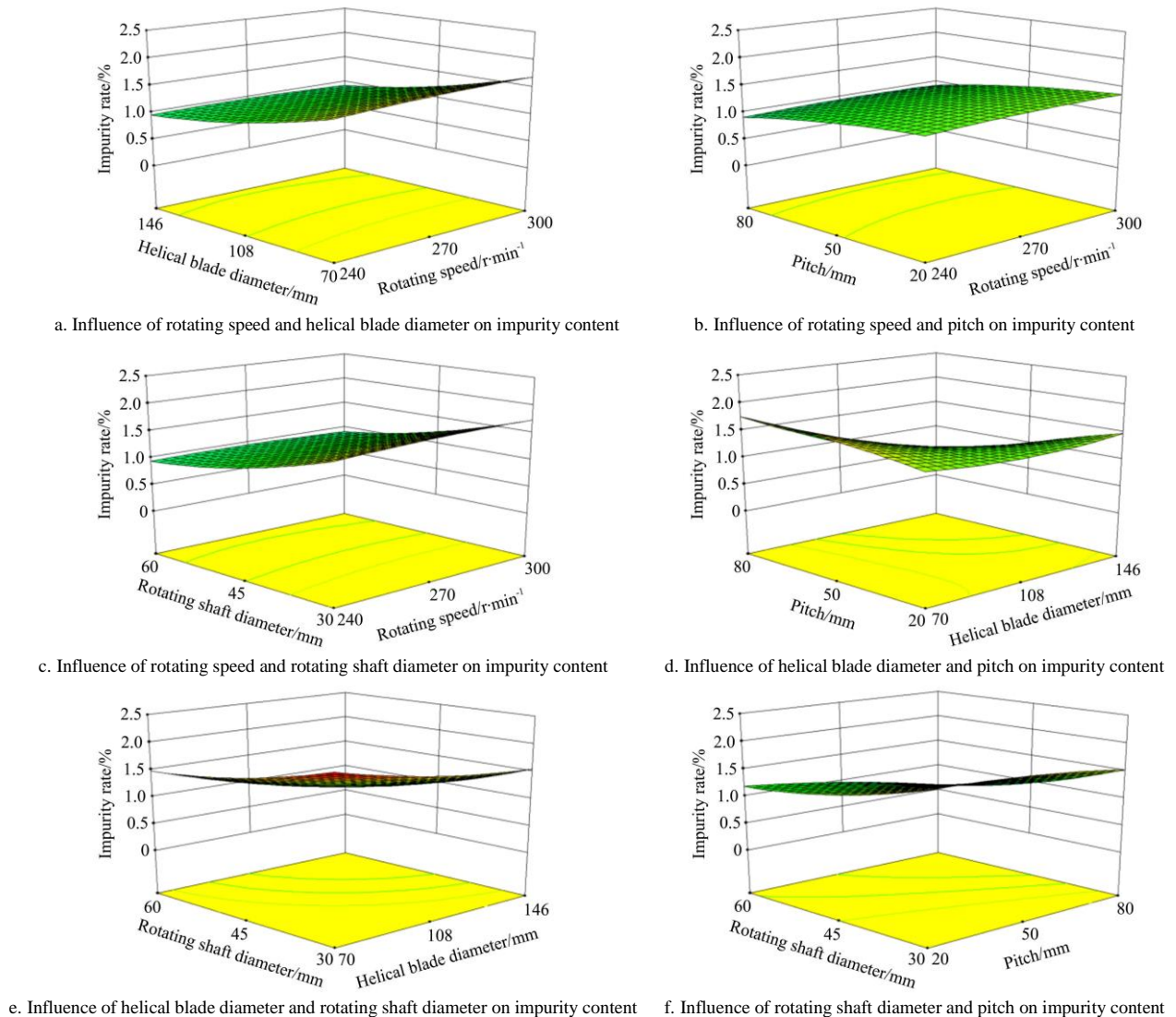
Figure 6   Influence of the interaction of factors on the impurity content

As shown in Figure 6a, the impurity content decreased with increasing helical blade diameter when the rotation speed was constant.   When the helical blade diameter was constant, the impurity content increased with increasing rotating speed.   This may be because the larger the helical blade diameter was, the smaller the gap between the helical blade and the sieve separator. The whole short stem was not easily deformed and separated from the sieve apertures, resulting in a decrease in impurity content. With increasing rotation speed, the interaction force between the rice grains and the short stems increased, and the motion orientation and deformation probability of the short stems impacted by grain flow increased.   As a result, stems can be easily separated from the sieve apertures, resulting in an increase in impurity content.   Figure 6b shows that the interaction between rotating speed and pitch had little effect on impurity content, and the effect of the other factor on impurity content was basically a constant trend when one of the factors was fixed.   As shown in Figure 6c, the impurity content decreased with increasing rotating shaft diameter when the rotating speed was constant.   When the rotating shaft diameter was constant, the impurity content increased with

increasing rotating speed.   This may be because the larger the rotating shaft diameter was, the smaller the space between the helical blade and the rotating shaft, and the trend of tilting or vertical posture of the short stem decreased.   As a result, it was not easy to separate stems from the sieve apertures, resulting in the reduction of impurity content.   As shown in Figure 6d, the impurity content was basically unchanged with increasing helical blade diameter when the pitch was constant.   When the helical blade diameter was constant, the impurity content increased with increasing pitch.   This may be because the larger the pitch was, the smaller the extruding effect of the spiral blade on the unit straw, which forced the short stems to be inclined or upright.   As a result, the stems can be easily separated from the sieve apertures, resulting in an increase in impurity content.   As shown in Figure 6e, the impurity content decreased with increasing helical blade diameter when the rotating shaft diameter was constant.   When the helical blade diameter was constant, the impurity content decreased with increasing rotating shaft diameter.   As shown in Figure 6f, the impurity content decreased with increasing rotating shaft diameter when the pitch was constant.   When the rotating shaft diameter

was constant, the impurity content was basically unchanged with increasing pitch.

To explore the best parameter combination of the screw conveyor, the experimental factors were optimized. The experimental factors and performance indicators need to meet certain constraints. Among them, the rotating speed should be maximized, which can not only improve the screening efficiency but also update the rice grains in the signal detection chamber in real time. The rotating shaft diameter should be minimized, which can not only increase the volume of rice grain but also decrease the weight of the screening and impurity removal device. The optimization goal was to minimize the impurity content, and the parameterized mathematical model was established as follows:

$$s.t.\begin{cases} \min y \\ \begin{cases} \max x_1 \\ \min x_4 \\ 240 \text{ r/min} \leq x_1 \leq 300 \text{ r/min} \\ 70 \text{ mm} \leq x_2 \leq 146 \text{ mm} \\ 20 \text{ mm} \leq x_3 \leq 80 \text{ mm} \\ 30 \text{ mm} \leq x_4 \leq 60 \text{ mm} \\ y > 0 \end{cases} \end{cases} \quad (9)$$

The multiobjective parameter optimization module of Design-Expert 8.0.6 software was used to optimize the mathematical model. The optimal parameters were obtained as follows: the rotating speed was 300 r/min; the helical blade diameter was 146 mm; the pitch was 80 mm; and the rotating shaft diameter was 30.6 mm. The impurity rate of the model prediction was 0.27%, and the reliability was 90%.

Through the Box Behnken experimental design, the influence of various factors on the impurity content was explored, to optimize the structure of the screening device and make its impurity content the lowest level. In order to explore the state of rice grain and short stem in the optimized screening device and the mechanism of impurity content, the material movement characteristics in the screening and impurity removal device will be analyzed.

3.2   Material movement characteristics in screening and impurity removal devices

To further analyze the motion distribution of the rice grains and short stems in the optimized screening and impurity removal device, the X-axis represents the axial direction of the screw transportation; the Y-axis and Z-axis represent the radial direction of the end face; and the coordinate origin is the connection point between the feed hopper and the screw conveyor when the particles flow steadily in the sieve separator under the action of the screw conveyor[29]. The sieve separator was divided into four areas: I, II, III and IV. The internal movement of the rice grains and short stems was dynamically simulated, as shown in Figure 7.
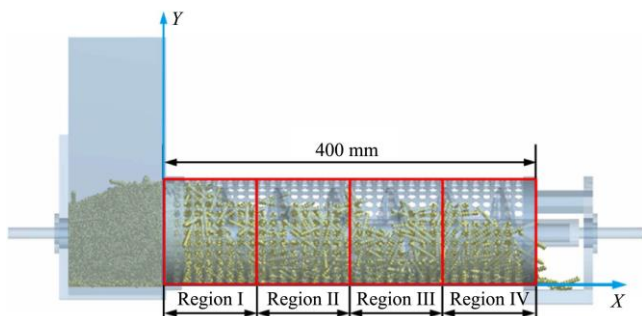

Figure 7   Regional division of the sieve separator

Figure 8 shows the number of rice grains and short stems in

each region under steady flow. As shown in Figure 8a, the number of rice grains in each region tended to be stable with time, which indicated that there was no congestion or accumulation of rice grains under the action of the screw conveyor. The overall design was stable. The number of rice grains in region I was the largest, and the numbers in region II and region III were close to 0, which indicated that the fall of rice grains from the sieve separator to the feeding hopper was mainly concentrated in region I. There was no rice grain in region IV, which indicated that the designed screening and impurity removal device could not cause entrainment loss of the rice grain. As shown in Figure 8b, the number of short stems in region I was stable at 300, and the number fluctuated greatly in regions II, III and IV, which indicated that the short stems fell with a certain randomness. In addition, there was a large difference in the number of short stems between region I and region II and between region II and region III, which indicated that short stems fell primarily between region II and region III. The number of short stems showed an overall downward trend with the change in the region, which indicated that some short stems fell prematurely from the sieve separator to the feeding hopper Which affected the detection accuracy of the moisture content.
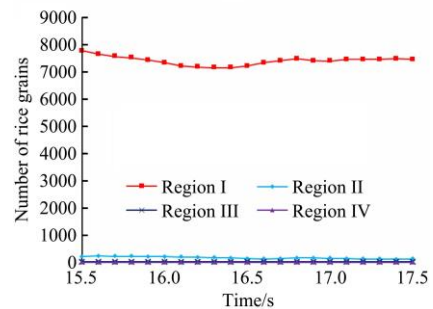
a. Number of rice grains in each region
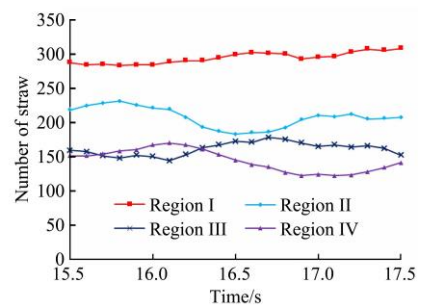
b. Number of short stems in each region

Figure 8   Contents of each region during steady flow

To clarify the motion mechanism of the short stem falling prematurely from the sieve separator and to explore the motion characteristics of the particles in each region of the screw conveyor as it rotated one cycle in the steady flow state, the macroscopic motion of the particle groups in each region of the screw conveyor movement was analyzed during two specific times for one cycle, as shown in Figure 9. As shown in Figures 9a and 9b, the rice grains and short stems in region I were extruded and mixed under the action of a screw conveyor and rotated in an orderly manner around the rotation direction. The overall distribution was more uniform in the circumferential direction. The rice grains were mainly concentrated on both sides and the bottom of the sieve separator and began to fall from the lower end of the sieve separator under the action of gravity. At this time, some of the short stems fell from the lower end of the sieve separator, and short stems also fell on the side of the sieve separator under the action of rotating force.

As shown in Figures 9c and 9d, there were still some rice

grains in region II, but the overall number was relatively small. The grains continued to be screened into the feeding hopper under the action of gravity.   The short stems cannot circulate around the screw conveyer.   At the top of the conveyor, a small number of short stems were driven to move around the circle, and the direction of motion was in the direction tangent to the circumferential motion, but the direction of the overall motion and attitude showed a disorderly trend.   A large number of short stems were mainly concentrated at the bottom and side of the sieve separator, which may be because a large number of rice grains and some short stems had fallen from the sieve separator in region I. The remaining rice grains and short stems cannot fully fill the sieve separator, resulting in insufficient circumferential friction between rice grains, short stems and the screw conveyor.   There was only the trend of radial movement, which led to the retention of a large number of short stems at the bottom and side of the sieve separator under the action of gravity and rotating friction.   This was also the main reason for the short stems falling prematurely from the sieve separator in region II.

a. Motion vector diagram of region I at 15.5 s time

b. Motion vector diagram of region I at 15.6 s time

c. Motion vector diagram of region II at 15.5 s time

d. Motion vector diagram of region II at 15.6 s time

e. Motion vector diagram of region III at 15.5 s time

f. Motion vector diagram of region III at 15.6 s time

g. Motion vector diagram of region IV at 15.5 s time

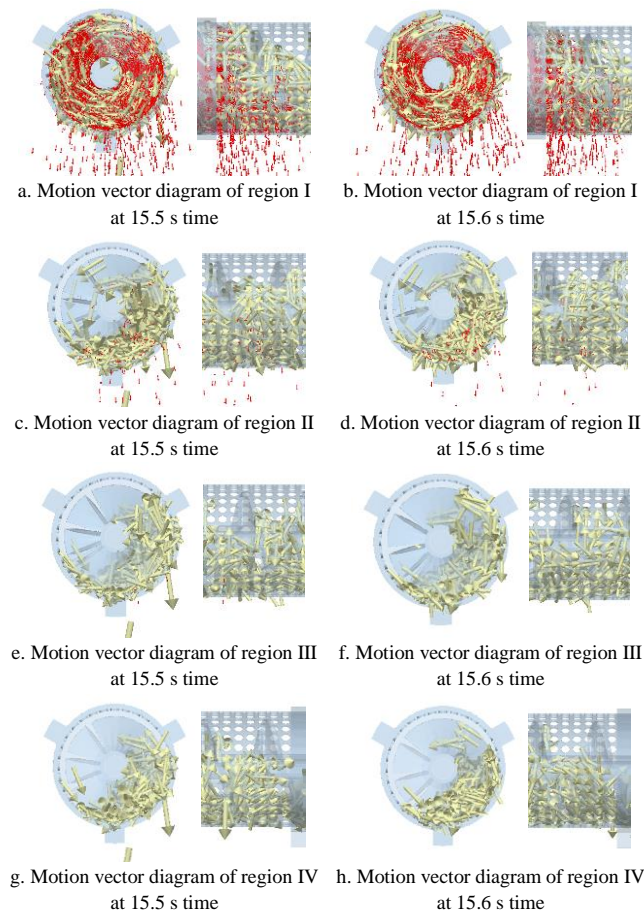h. Motion vector diagram of region IV at 15.6 s time

Figure 9   Motion vector diagram of particle groups in each region

As shown in Figures 9e and 9f, there were almost no rice grains in region III, which also verified the accuracy of the grain number statistics in each region during the steady flow in Figure 8. At this time, due to the action of the screw conveyor and gravity, the short stems underwent unsteady flow in the sieve separator, and the direction and orientation of movement were disorganized.   A small number of short stems fell from the sieve separator and were mainly concentrated at the bottom.   This may be due to the lack of friction with the screw conveyor because the short stems could not rotate in the circumferential direction, and the radial distance of the sieve separator was large, which can only change the direction and orientation of the short stems while driving the radial movement of

the straw.   There was a certain probability that the short stems fell vertically from the sieve separator when gravity played a dominant role.

As shown in Figures 9g and 9h, the materials in region IV were all composed of short stems, and the number of rice grains was reduced to 0.   Compared with region III, the circumferential distribution of short stems in the sieve separator was smaller, and a small number of short stems still fell from the sieve separator under the action of gravity.   However, there were fewer short stems falling prematurely in this area.   The main reason was that the short stems were pushed to the end of region IV under the action of the radial force of the spiral conveyer, and the short stems had little chance of undergoing great change in orientation.

The regional particle motion vector diagrams cannot fully characterize the particle flow process in the sieve separator, and the particle velocity in different axial positions also showed some differences.   The axial component and average velocity distribution of particles in each region along the X-axis are shown in Figure 10.   As shown in Figure 10a, the speeds of rice grains and short stems were the same in region I, which indicated that a large number of rice grains and short stems moved as a group in region I.   The axial component of the average velocity of rice grains increased gradually in region I and region II and then decreased gradually.   This was mainly due to the radial transport of rice grains by screw conveyors in region I and region II and the collisions and friction between a large number of short stems and rice grains.   The gradual decrease in the speed after regional II may be because a large number of rice grains fell from the sieve separator until there were no rice grains in region IV, which resulted in a radial velocity of 0.   The average velocity of short stems in the axial component increased gradually in region I and region II.   The speed in region III and region IV tended to stabilize at first and then increased gradually.   This may be because there was a large number of short stems and grains at the beginning of migration.   This led to the circumferential movement of the short stems along with the screw conveyor in the circumferential direction and causes some short stems to lag and slip to a certain extent.   With the continuous axial movement of the short stems, some of the short stems gradually fell in the sieve separation drum so that they could not move in the circumferential direction, and a large number of short stems could only accumulate at the bottom and side of the sieve separator.   Under the action of the screw conveyor, there was only axial motion, which led to a certain upward trend of the speed of the short stems as a group.

As shown in Figure 10b, the average speed of the rice grains was higher than that of the short stems in regions I, II and III. This was mainly due to the large size of the short stems, and their movement mainly depended on friction with the screw conveyor. The size of the rice grains was small.   The mutual extrusion and friction of rice grains among rice grains, between rice grains and short stems, and between rice grains and screw conveyors can easily change the speed and amount of movement of the rice.   At the same time, the rice can pass through the gaps between short stems by the action of gravity.   The overall trend was basically consistent with the component of the X-axis, but the overall value was large.   This is mainly because the average velocity not only had a component in the X-axis but it also had circumferential velocity of rotation.   The average speed of the short stems overall gradually decreased.   This was mainly due to the circumferential motion of the short stems in region I.   The number of rice grains and short stems gradually decreased with axial migration, and the

trend of circumferential circulation of the remaining short stems became increasingly weaker.   Therefore, the average speed of the short stems decreased gradually.

a. X-axis component of the average particle velocity

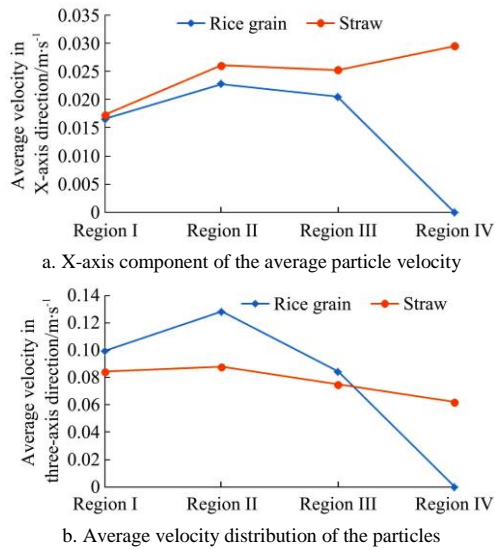b. Average velocity distribution of the particles

Figure 10   Particle velocity distribution in the sieve separator

### 3.3   Comparative results of field experiments

The comparison of the impurity content of rice before and after screening is shown in Table 5.

Table 5   Comparison of the impurity content of rice before and after screening

Date	Time	Impurity content before screening I_1/%	Impurity content after screening I_2/%	Effective screening rate S/%
Day 1	8:00	2.92	0.37	87.33
	10:00	2.80	0.34	87.86
	12:00	3.22	0.29	90.99
	14:00	2.75	0.37	86.55
	16:00	2.83	0.34	87.99
	18:00	2.60	0.26	90.00
Day 2	8:00	2.98	0.29	90.27
	10:00	3.11	0.37	88.10
	12:00	2.76	0.33	88.04
	14:00	2.74	0.31	88.69
	16:00	2.64	0.28	89.39
	18:00	2.58	0.28	89.15
Day 3	8:00	2.75	0.34	87.64
	10:00	2.66	0.32	87.97
	12:00	2.63	0.31	88.21
	14:00	2.71	0.29	89.30
	16:00	2.83	0.31	89.05
	18:00	2.61	0.28	89.27
Day 4	8:00	2.58	0.28	89.15
	10:00	2.64	0.33	87.50
	12:00	2.37	0.29	87.76
	14:00	2.50	0.29	88.40
	16:00	2.48	0.31	87.50
	18:00	2.65	0.26	90.19

Table 5 shows that the range of impurity content of screened rice was 0.26% to 0.37%, and the maximum difference between the results for the screened rice and the predictions of the model was 0.10%.   There may be some variations and errors in the moisture content of rice due to the temperatures and humidities of the air on different days.   The prediction model was accurate and reliable within the allowable range of error.   In addition, the range of impurity content of rice before screening was from 2.60% to 3.17%.   The impurity content decreased significantly, and the maximum

effective screening rate was 90.99% after processing with the screening device.   The results showed that the optimized screening and impurity removal device can effectively reduce the impurity content of rice.   To explore the effect of screening and impurity removal devices on the determination of rice moisture content, the results of the online moisture content detection device for rice, without and with processing by screening and impurity removal devices, were compared with the moisture content measured by the 105°C drying method.   The results are shown in Figure 11.

a. Day 1

b. Day 2

c. Day 3

d. Day 4
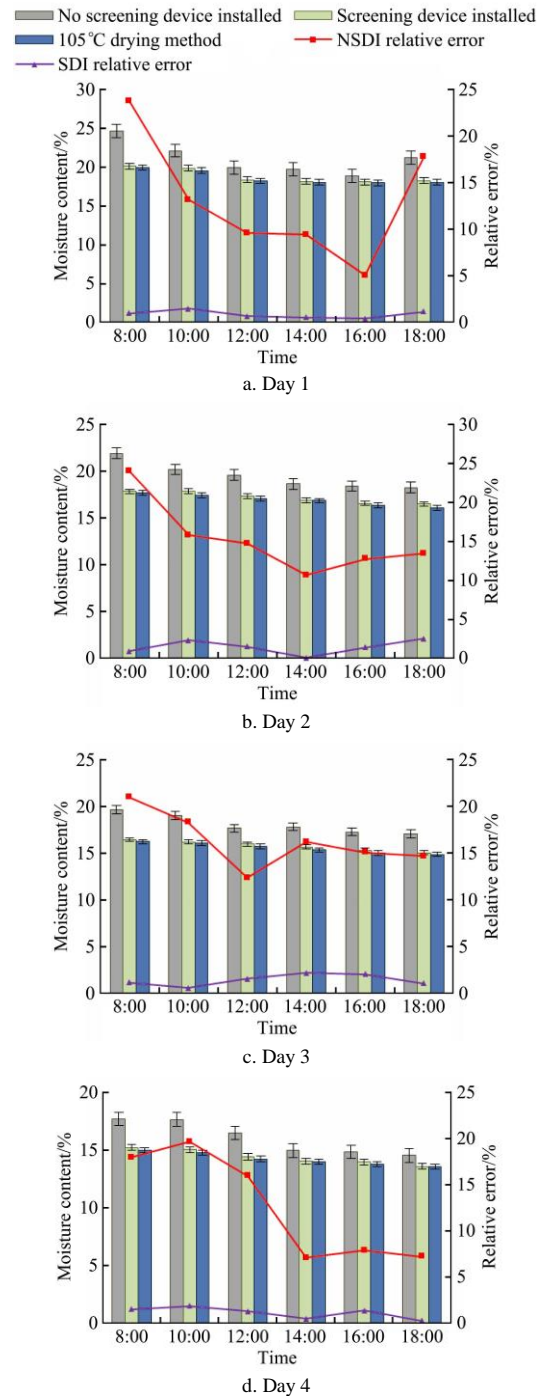
Note: NSDI: No screening device installed; SDI: Screening device installed.

Figure 11   Comparative of the determination of moisture content

As shown in Figure 11, the moisture content of rice grains decreased gradually with the passage of time in a day.   This was mainly due to the late ripening effect of rice grains on stems, and the moisture content of rice grains decreased gradually with increasing light intensity.   With increasing date, the grain moisture

content of rice decreased gradually. In addition, based on the 105°C drying method, the results of the online moisture content detection device for rice that had not been processed with the screening and impurity removal device were larger (and were too high) than those for rice that had been screeded and its impurities had been removed. There was no screening or impurity removal device installed to directly detect the moisture content, and there was a large number of short stems with the rice in the grain tank. The moisture content of rice grains with short stems was much higher than that of rice grains at the harvest time, which led to the detection of an overall higher moisture content. The error of the determination of the moisture content detected by the online detection device installed with the screening and impurity removal device was significantly reduced, and the error range was 0.12% to 2.55%, which showed that the installation of the screening and impurity removal device had a significant effect on improving the accuracy of the online moisture content detection device. At the same time, when the screening and impurity removal device was not installed, the error in the measurement of moisture content by the online detection device decreased gradually with increasing data. This may be due to the higher moisture content at the beginning of harvest, which resulted in a higher impurity content in rice grains after harvest, and the impurity content also affected the accuracy of moisture content detection. The results showed that moisture content and impurity content influenced and restricted each other. In the future, the interaction mechanism between the moisture content and impurity content will be deeply analyzed to provide a theoretical reference for the research and optimization of accurate detection equipment for moisture content. Additionally, the results of this study can effectively guide the timely harvest operation and the appropriate allocation of harvesting machinery and improve the intelligence of agricultural machinery and the accurate management of agricultural production.

In this study, Longjing 29 rice widely planted in Northeast China was taken as the research object, and a screening and impurity removal device was developed according to its physical characteristics, which provided theoretical guidance for accurate monitoring of moisture content. However, there are significant physical differences among different varieties of rice, such as "long grain type", "short grain type" and "flat grain type"[30]. In the later stage, the differences of different grain types will be counted, and the screening and impurity removal devices suitable for different varieties will be designed according to their physical characteristics. In addition, although the on-line moisture content detection device met a certain detection accuracy, there was still a certain error. In this paper, the motion characteristics of rice grains and short stems in the screening device were explored through simulation analysis, which provided a reference for further optimizing the shape and size of the screening device in the later stage. Such as setting special-shaped holes in different areas and changing spiral diameter.

Although the motion mechanism of the material was analyzed from the aspects of density distributions, motion and orientation, and characteristics of the grain in the sieve separator, only the optimized structural parameters of the screw conveyor were explored. There was no quantitative comparison carried out to describe the mathematical relationship between the material and the sieve separator with different structural parameters. There was no in-depth analysis of the influence mechanism between impurity content and moisture content. Limited to the length of the article, this study does not list and analyze the motion characteristics of

materials in the screening and impurity removal device with different parameters, and does not feed them back to the optimal design of key structures and parameters of the device. In the later stage, the screening and impurity removal device will be further optimized and designed according to the feedback results of simulation and field experiment. In addition, based on the mathematical relationship between multivariable fitting and grain moisture content, we will focus on exploring the interaction mechanism between impurity content and moisture content to provide a theoretical basis for the accurate determination of moisture content. At the same time, this work provides a data reference for the accurate determination of impurity content under different moisture content conditions.

4   Conclusions

In this study, the key components of the screening and impurity removal device were designed, and the optimal combination parameters and screening mechanism were explored through simulation test and Box-Behnken response surface method. The conclusions are as follows:

(1) When the rotating speed was 300 r/min, the diameter of spiral blade was 146 mm, the pitch was 80 mm, the diameter of rotating shaft was 30.6 mm, and the minimum impurity content was 0.27%.

(2) The particle flow density of the optimized screening and impurity removal device gradually decreased with region increasing, and the falling of grains and short stems were mainly distributed in region II and region III.

(3) The results of field experiment showed that the impurity content after screening ranged from 0.26% to 0.37%, and the maximum effective screening rate was 90.99%. The error of moisture content detected by the on-line detection device installed with screening and impurity removal device was significantly reduced, and the error range was 0.12%-2.55%.

(4) This study provides methods and ideas for the online accurate detection of moisture content and provides a reference for the research and simulation of related screening devices.

Acknowledgements

[References]

[1] Ozbekova Z, Kulmyrzaev A. Study of moisture content and water activity of rice using fluorescence spectroscopy and multivariate analysis. Spectrochimica acta, Part A. Molecular and biomolecular spectroscopy, 2019; 223: 117357. doi: 10.1016/j.saa.2019.117357.

[2] Zheng B, Wang H, Shang W, Xie F, Li X, Chen L. Understanding the digestibility and nutritional functions of rice starch subjected to heat-moisture treatment. Journal of Functional Foods, 2018; 45: 165–172.

[3] Jain S, Mishra P K, Mishra J, Thakare V V. Design and analysis of H-shape patch sensor for rice quality detection. Materials Today: Proceedings, 2018; 29: 581–586.

[4] Keiji T, Yasuaki M, Yuta N, Ryota I, Kayo F, Kenji S. Magnetic method for measuring moisture content using diamagnetic characteristics of water. Meas Sci Technol, 2017; 28(1): 014010. doi: 10.1088/1361-6501/28/1/014010.

[5] Pathaveerat S, Pruengam P. Low cost measurement of moisture content in long grain paddy. Journal of Stored Products Research, 2020; 89: 101728. doi: 10.1016/j.jspr.2020.101728.

[6] Julrat S, Trabelsi S. In-line microwave reflection measurement technique for determining moisture content of biomass material. Biosyst Eng, 2019; 188: 24–30.

[7]   Liu J X, Liu T, Mu G Q, Chen J H.   Wavelet based calibration model building of NIR spectroscopy for in-situ measurement of granule moisture content during fluidized bed drying.   Chem Eng Sci, 2020; 226: 115867. doi: 10.1016/j.ces.2020.115867.

[8]   Vera Zambrano M, Dutta B, Mercer D G, MacLean H L, Touchie M F. Assessment of moisture content measurement methods of dried food products in small-scale operations in developing countries: A review. Trends Food Sci Technol, 2019; 88: 484–96.

[9]   Figueiredo Neto A, Cárdenas Olivier N, Rabelo Cordeiro E, Pequeno de Oliveira H.   Determination of mango ripening degree by electrical impedance spectroscopy.   Comput Electron Agric, 2017; 143: 222–226.

[10] Raja V, Shanmugasundaram S.   Development of capacitance based nondestructive ripening indices measurement system for sapota (Manilkara zapota).   J Food Process Eng, 2020; 43(3): e13307.   doi: 10.1111/jfpe.13307.

[11] Liu D, Wang E, Wang G, Wang P, Wang C, Wang Z.   Non-destructive sugar content assessment of multiple cultivars of melons by dielectric properties.   J Sci Food Agric, 2021; 101(10): 4308–4314.

[12] Wang R, Wang D, Ren X, Ma H.   Nondestructive detection of apple watercore disease based on electric features.   Transactions of the CSAE, 2018; 34(5): 129–136. (in Chinese)

[13] Besharati B, Lak A, Ghaffari H, Karimi H, Fattahzadeh M.   Development of a model to estimate moisture contents based on physical properties and capacitance of seeds.   Sensors Actuators, A Phys, 2021; 318: 112513. doi: 10.1016/j.sna.2020.112513

[14] Wang J W, Tang T Y, Tang H, Xu C S, Zhou W Q, Wang Q.   Design and experiment of on-line detection device for capacitive paddy rice moisture content of combine harvester.   Transactions of the CSAM, 2021; 52(3): 143–52. (in Chinese)

[15] Mai Z, Li C, Xu F, Fang Z.   Design and test of grain moisture online measuring system based on floating ground capacitance.   Transactions of the CSAM, 2014; 45(10): 207–213. (in Chinese)

[16] Wan L, Tang H Y, Ma G Y, Che G, Zou D D, Sun W S.   Optimization design and experiment on finned double plates rice moisture content measuring device.   Transactions of the CSAM, 2021; 52(2): 320–328. (in Chinese)

[17] Zhang B H, Qian C Q, Jiao J K, Ding Z H, Zhang Y, Cui H G, et al.   Rice moisture content detection method based on dielectric properties and SPA-SVR algorithm.   Transactions of the CSAE, 2019; 35(18): 237–244. (in Chinese)

[18] Liang Z, Xu L, Baerdemaeker J De, Li Y, Saeys W.   Optimisation of a multi-duct cleaning device for rice combine harvesters utilising CFD and

experiments.   Biosyst Eng, 2020; 190: 25–40.

[19] Jia H L, Deng J Y, Deng Y L, Chen T Y, Wang G, Sun Z J, et al.   Contact parameter analysis and calibration in discrete element simulation of rice straw.   Int J Agric & Biol Eng, 2021; 14(4): 72–81.

[20] Roessler T, Katterfeld A.   DEM parameter calibration of cohesive bulk materials using a simple angle of repose test.   Particuology, 2019; 45: 105–115.

[21] Zhang S, Tekeste M Z, Li Y, Gaul A, Zhu D, Liao J.   Scaled-up rice grain modelling for DEM calibration and the validation of hopper flow. Biosyst Eng, 2020; 194: 196–212.

[22] Wu X J, Tang N, Liu B, Long Z L.   A novel high precise laser 3D profile scanning method with flexible calibration.   Opt Lasers Eng, 2020; 132: 105938.   doi: 10.1016/j.optlaseng.2019.105938

[23] Zhou L, Yu J Q, Wang Y, Yan D X, Yu Y J.   A study on the modelling method of maize-seed particles based on the discrete element method. Powder Technol, 2020; 374: 353–376.

[24] Jiang Z, Du J, Rieck C, Bück A, Tsotsas E.   PTV experiments and DEM simulations of the coefficient of restitution for irregular particles impacting on horizontal substrates.   Powder Technol, 2020; 360: 352–365.

[25] Wang Q R, Mao H P, Li Q L.   Modelling and simulation of the grain threshing process based on the discrete element method.   Comput Electron Agric, 2020; 178: 105790.   doi: 10.1016/j.compag.2020.105790.

[26] Zhang R F, Jiao W, Zhou J L, Qi B, Liu H, Xia Q Q.   Parameter calibration and experiment of rice seeds discrete element model with different filling particle radius.   Transactions of the CSAM, 2020; 51(S1): 227–235. (in Chinese)

[27] Xu L, Li Y, Sun P, Pang J.   Vibration measurement and analysis of tracked-whole feeding rice combine harvester.   Transactions of the CSAE, 2014. (in Chinese)

[28] Wu W F, Chen J Y, Cheng R M, Jin Y, Wei X S, Xiao B L, et al. Coupling relationship between content of unsaturated fatty acid and drying system of corn grain after variable temperature and humidity drying. Transactions of the CSAE, 2019; 35(16): 328–333. (in Chinese)

[29] Liu Y, Han Y L, Jia F G, Yao L N, Wang H, Shi Y F.   Numerical simulation on stirring motion and mixing characteristics of ellipsoid particles.   Acta Phys Sin, 2015; 64(11): 114501.   doi: 10.7498/ aps.64.114501.

[30] Wang J W, Xu C S, Xu Y N, Wang Z M, Qi X, Wang J F, et al. Influencing factors analysis and simulation calibration of restitution coefficient of rice grain.   Appl Sci, 2021; 11(13): 5884.   doi: 10.3390/ app11135884.